Combining Haptic Sensing with Safe Interaction

Martin Battaglia, Laurent Blanchet, Abderrahmane Kheddar, Suuji Kajita and Kazuhito Yokoi

Abstract— We propose a solution which combines haptic sensing with safe interaction, at low cost. Contact locations are made through a flexible sheet of tactile binary switch matrix. This sheet covers the surface of a rigid bumper module assembled to the robot's basic link through a distributed pressure sensing units. Combination of location and force provides the haptic sensing module. The haptic system is covered with a flexible outer material which role is to absorb contact impacts and to cast local surface profile on which the robot can take support. This overall system allows having a combined haptic sensing with safe and robust physical interaction with both the environment and the human using active compliance. We discuss the benefit of such a simple and modular concept and present how to design the cover material. A simple prototype is realized and experienced.

I. INTRODUCTION

Haptic sensing and safe interaction with the environment and humans are two challenging issues in robotics in general, and in humanoid robots in particular. These issues are crucial and even interrelated when humanoid robots are allowed to take contact supports with entire body on any part of the environment. This example highlights the importance for the robot to know where contacts occurred on its body and what is the total force wrench applied on each of its links, it also bring to light the importance to have robust contact formation for a stable whole-body motions support; see a thorough discussion of this example in [1].

Recent researches are tackling the problem of haptic sensing through bio-mimetic approaches (artificial skin). These approaches are interesting and challenging; several admirable technologies and designs have been proposed to build an artificial sensing skin. However, we distinguish between haptic sensing that is used for whole-body motions, interaction and closed-loop task realization, from that haptic sensing used for robot perception and acquisition of haptic knowledge or precise dexterous manipulation. There are also considerable works in achieving human-robot safety collocated physical human-robot interaction through various techniques that can be gathered in two main categories: active, passive or hybrid compliance. Several very sophisticated design and prototypes

have been recently demonstrated with very impressive results.

Our work aims at designing a combined haptic sensing and active safety interaction system which can cover the entire body of the robot for whole body motion and at low cost. It will be used for detecting, locating and absorbing safely the contacts and the collisions of both the (humanoid) robot and its surrounding. Such a combined system is very useful for a humanoid robot operating in a changing environment where objects and possibly human beings are moving. The total humanoid's cover surface is important enough for parameters such as cost, weight, and thickness to be critical.
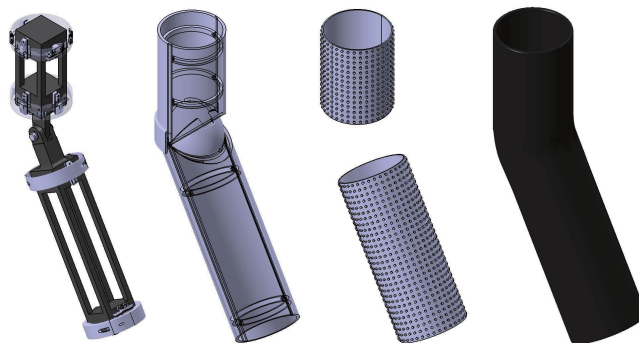

Fig. 1.   Exploded view of the whole design for an arm, from left to right: the robot links (dark) and the distributed pressure sensors (gray rings), the bumper, the contact location tactile binary switches, the compliant cover.

Our approach is driven by practical viewpoints, as will be seen later on, some researches have taken more or less a similar path considering similar constraints. We simply went a bit further in our investigations to see how a combined whole-body haptic and safe interaction can be tackled with a pragmatic way for real usage and applicability. We consider any link of the robot to be made of two main parts: (i) the proper robot link, and (ii) our system; the later consists in four parts, Fig. 1: (ii) a simple shape bumper surrounding the robot's link and attached to it through (i) distributed pressure sensor units; (iii) a contact location sensor, being a thin sheet of matrix tactile binary switches (in its simplest form), and which covers entirely the bumper: its role is to provide contact locations (contact surfaces and their barycenter), and (iv) a compliant material (foam) covering the tactile sheet which role is to well cast the contacting surface and to absorb chocks at the contact spots.

The first part of the paper discusses the overall concept; the second part focuses on a computation tool allowing to determine the characteristics of the compliant outer cover; the third part presents a preliminary proof-of-concept.

II. Proposed Solution

Our solution combines whole-body haptic sensing and safety interaction function. The requirements that drove our approach are summarized as follows:

- coverage of wide areas of robot's links with minimum signal processing, latencies, and data flow on the robot's network or bus;
- usage of a flexible outer cover to absorb impacts due to desired or not desired contacts, and to locally cast surface profile; it can also be used for aesthetics;
- location, on the robot, of contact areas and measurement of force wrenches per link;
- modular, quickly demountable, interchangeable with an easily maintenance and life cycle;
- not costly, light and with reasonable thickness

We devised a modular system which allows combining simple technologies in a multilevel design described in Fig. 1. Starting from a bare robot's link, we attach to it a rigid simple shaped cover (bumper) through distributed pressure units which deformation measures the resultant force wrench acting on the link. Distributing pressure units on the link is preferable to having a single location of force measure e.g. using a commercial 6dof force sensor. Yet, an optimal distribution and location is to be found for each link by restricting the number of the pressure units (if possible to 6 or less). This part will be published in another paper.

The bumper is covered by a flexible tactile sensing sheet, see Fig. 1. Its role is to sample the contact spots on each link. That is, where contacts occur and, for each contact, an estimate of its area and barycenter. Our choice would have been to use flexible keyboards technology, since it is simple, mature and cheap enough. But the switches are mechanical whereas capacitive switches may have superior advantages. Other options are possible. In [2], a sensitive skin is developed on the basis of single sided electrode units covered by a conductive rubber with a resistivity which depends on the applied pressure. Their matrix tactile system needs one wire per taxel and could basically be used in our case. In [3] a multi-contact detection sensor sheet based on resistive measurement consists in two conductive plates each in a discrete combination of parallel conductive bands are separated by a pressure sensitive material that acts as an electrical insulator under no load but conduct electricity when pressure is applied. The material is chosen for its electric characteristics and the thickness being a result of the fabrication process. If bended in a low curvature, it could be damaged. The work by [4] uses the same physical principle for measuring the pressure distribution, but with a grid architecture, what reduces the number of wires to one per line and one per column. Using the same kind of conductive rubber, the system shown in [5] goes further in the reduction of the wires number by using electrical impedance tomography that allows measurement only on the borders of the skin to obtain pressure distribution and can basically be used in our design. Since we consider pressure sensor units to have the resultant force wrench on each link, quantifying the pressure information is not necessary in our case. That is why we can certainly make previous technologies simpler or thinner, or make use of binary on/off switches. It is what we did for the proof-of-concept, with putting a diode after each switch to avoid ghosting effect. There are obviously several additional technologies which we did not mention not only because of space but also because they are not mature enough for use. We are however investigating capacitive switches.

At this stage we have the choice between designing the tactile sensor with (i) thick resistive or capacitive foam so that the tactile sensor could also absorb impacts, or (ii) a thin tactile sensor and a separate additional flexible cover to absorb impacts. We decided to win the second choice for many reasons. Among which, the freedom to design the sensor with optimal resolution using best of resistive and capacitive material layers, avoid using stretchable technologies for the tactile sensor since they compose the surface of the link, protect the sensor by its inner location possibility i.e. between the bumper and the flexible cover, design the cover with esthetic shapes, etc.

Once the tactile sensor technology is decided, it is covered by a flexible material which role is to absorb impacts during the necessary time to detect it and react to it (active compliance), and also to cast well the surface to build robust whole-body motion supporting contacts. This part is very important and need to be carefully designed. Authors in [6] considered criteria borrowed from human injury data and tested impact with different materials. Recent researches make use of data from crash-tests in automobile industry [7]. But to our best knowledge, the model for mechanical characteristics and the thickness determination of the cover has not been thoroughly studied. This paper focuses on computation of the thickness for a given material or on characterizing the material both under constraints related to the issue of haptic sensing and safe interaction. We also study the influence of the flexible cover's thickness and the resolution on the sensitivity of the tactile sheet.

III. Flexible cover's characteristics

We based our characterization of the cover on the excellent review of the impact problem performed by Stronge [8]. We build a method for computing the material properties of a cover given a set of well defined constraints. First, we define a set of relations linking several parameters involved in the characterization of the cover's material. Only after, we explain the algorithm which makes use of these relations in an interactive design process.

Consider two bodies B and B' for which the following parameters can be defined. The effective modulus: $E_* = \left[\left(1 - v_B^2\right) E_B^{-1} + \left(1 - v_{B'}^2\right) E_{B'}^{-1}\right]^{-1}$ where E_i is the Young's modulus (Pa) and v_i the Poisson's ratio of the body i; the effective radius: $R_* = \left[R_B^{-1} + R_{B'}^{-1}\right]^{-1}$ where R_i is the local radius of curvature of the body i (m) at the contact point; the effective mass: $m_* = \left[m_B^{-1} + m_{B'}^{-1}\right]^{-1}$ where m_i is the contact projected mass of the body i.

The collided body, B', is the obstacle and its mechanical characteristics are considered known (worst case setting). We

want here to cover the colliding robot body B with a flexible material, whose goal is to absorb the impact during the time needed to detect and to react (computation of the active compliance), which is a given time constraint τ (seconds).

A. Impact model

In chapter 6 of [8], Stronge established the impact model for free colliding spherical bodies; we followed similar computation steps for establishing an impact model that would apply for the system represented in Fig. 2. It is a 1dof robotic motorized link, covered by elastic foam and for which we establish the impact model in the worst case, i.e. when it hits a rigid, unmovable obstacle like a wall corner.
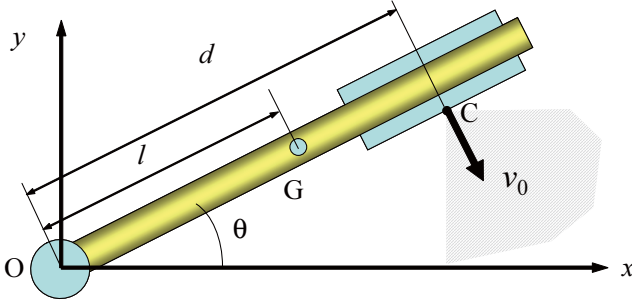

Fig. 2. Illustration of the prototype case study.

In this simple case study, C is the contact point, G the center of mass, O the origin, d the distance between the contact point and the origin, l the distance between the center of mass and the origin, and θ the joint angle of the arm. The dynamic model for the arm is:

$$J\ddot{\theta} + Mgl\sin\theta = u - dF \quad (1)$$

where $J = \frac{m_B}{12}(3R_B^2 + d^2) + m_B l^2$ is the moment of inertia, u the motor torque, and $F = K_s\delta^{3/2}$ the contact force, with $K_s = \frac{4}{3}E_*R_*^{1/2}$ [8]. The relations $\ddot{\theta} = \frac{\ddot{\delta}}{d}$ and $\theta - \theta_0 = \frac{\delta}{d}$ lead to:

$$\frac{J}{d}\ddot{\delta} + Mgl\sin\left(\theta_0 + \frac{\delta}{d}\right) = u - dK_s\delta^{3/2} \quad (2)$$

where θ_0 the angle of the arm at the contact. Considering that $\ddot{\delta} = \dot{\delta}\frac{d\dot{\delta}}{d\delta}$ and the initial conditions $\dot{\delta}(0) = -v_0$ and $\delta(0) = 0$, the integration of the previous equation gives:

$$\frac{J}{2d}(\dot{\delta}^2 - v_0^2) - Mgld\cos\left(\theta_0 + \frac{\delta}{d}\right) = u\delta - \frac{2dK_s}{5}\delta^{5/2} \quad (3)$$

When the compression phase ends, at $t = t_c$, the normal relative velocity vanishes, so $\dot{\delta} = 0$, $\delta = \delta_c$, and as $\delta << d$, $\cos\left(\theta_0 + \frac{\delta}{d}\right) \approx \cos\theta_0$. The eq. (3) gives us the expression of the compression time:

$$t_c = \int_0^{\delta_c}\left(v_0^2 + \frac{2d^2}{J}Mgl\cos\theta_0 + \frac{2du\delta}{J} - \frac{4K_sd^2}{5J}\delta^{5/2}\right)^{-1/2}d\delta \quad (4)$$

and becomes:

$$\frac{J}{2d}v_0^2 + Mgld\cos(\theta_0) = -u\delta_c + \frac{2dK_s}{5}\delta_c^{5/2} \quad (5)$$

None of these two equations has an analytical solution, so we can not find an analytical expression of E_* in function of t_c as done in the Stronge's example.

B. Yield aspect

Whatever material we choose, we will forbid to reach the plastic domain during compression so that the impact does not become rigid. This second part is in quasi-static and the results depend of the material and the geometry, not of the mechanical structure and the dynamics of the robot. The effective modulus gives us the ratio $\frac{E_B}{1-v_B^2}$, what we use to choose a material and so to obtain Y_B, the yield stress of the body B (Pa). The transition contact pressure between the elastic and the plastic domains is $p_Y = v_Y Y_B$. It occurs for the body B at the indentation limit for elastic deformation δ_Y obtained from:

$$\frac{p_Y}{Y_B} = v_Y = \frac{4E_*}{3\pi Y_B}\sqrt{\frac{\delta_Y}{R_*}} \quad (6)$$

where the ratio v_Y depends on the geometry of the contact (for example, for a contact between two spheres: $v_Y = 1.1$ and between a cylinder and a plane: $v_Y = 1.5$). This leads to the non-dimensional indentation $\frac{\delta_Y}{R_*}$ required to initiate yield, a material property:

$$\frac{\delta_Y}{R_*} = \left(\frac{3\pi}{4}\right)^2\left(\frac{v_Y Y_B}{E_*}\right)^2 \quad (7)$$

We do not make use of eq. (7) explicitly, it is checked at each step of the design process to ensure that the indentation do not reach the yield limit.

C. Skin thickness for energy absorbing

Let U_r be the material resilience which defines the energy that the material can elastically absorb per unit of volume. We know that a sphere/cylinder contact (our case study), is elliptic and can be expressed, according to Hertz's contact theory as $S_c = 1.3\pi\left(\frac{FR_*}{E_*}\right)^{2/3}$. Finite element simulations show that volume absorbing the energy can be approximated by a cylinder with a surface 4 times bigger in both dimensions than the contact area, i.e. $16S_c$, the thickness e being its height.

Considering the energy absorption rate linear leads to the energy to be absorbed by the skin: $E_n = E_k \cdot (t_0/t_c)$, with t_c the time that would have been required if the skin had to absorb all the impact as defined before. W is the work done by the contact effort and we state that all of the energy is transmitted to the material (again, worst case scenario) so $W = E_n$. Stronge's work [8] gives us: $\frac{W}{E_*R_*^3} = \frac{8}{15}\left(\frac{\delta}{R_*}\right)^{5/2}$ thus the effort : $F = \left(\left(\frac{8}{15}\right)^2 E_k^3 E_*^2 R_*\right)^{1/5}$.

The resilience U_r is given by $U_r = \frac{Y_B^2}{2E_B}$. Considering that $U_r e 16S_c = E_n$, and that $E_k = \frac{1}{2}mv_0^2$, we have:

$$e = \frac{m^{3/5} \cdot v_0^{6/5} \cdot (t_0/t_c)}{84 \cdot U_r \cdot \left(R_*^2 E_*^{-1}\right)^{6/15}} \quad (8)$$

D. Sensitivity of the sensor

We will use a sensor build as a square matrix of switch. As this sensor does discrete contact detection, it is important to estimate the sensitivity of the sensor, i.e. the necessary contact force to be detected, considering the thickness and the resolution of the matrix, i.e. distance between two switches.

We based our study on [9] (Chapt. 3). We consider a semi-infinite, homogeneous, linear elastic, incompressible (i.e. with a Poisson ratio of 0.5) material, on which a normal punctual force F is applied. We define σ_z the stress in the normal direction of a given point. This model states:

$$F = \frac{2\sigma_z \pi (x^2 + y^2 + z^2)^{5/2}}{3z^3} \quad (9)$$

where (x,y,z) are the coordinates of a point relative to the contact point, the contact point being the origin. In the worst case, i.e. the contact point being equidistant of each switch, we set the point on the center of the switch. There, we have $\sigma_z = \frac{F_s}{S}$, where F_s is the necessary force to press the switch until the electrical contact and S the surface of the contact between the switch and the cover, $x^2 + y^2 = \frac{d^2}{2}$, d being the resolution of the matrix and $z = e$, e being the thickness of the skin. We obtain:

$$F = \frac{2F_s \pi (\frac{d^2}{2} + e^2)^{5/2}}{3Se^3} \quad (10)$$
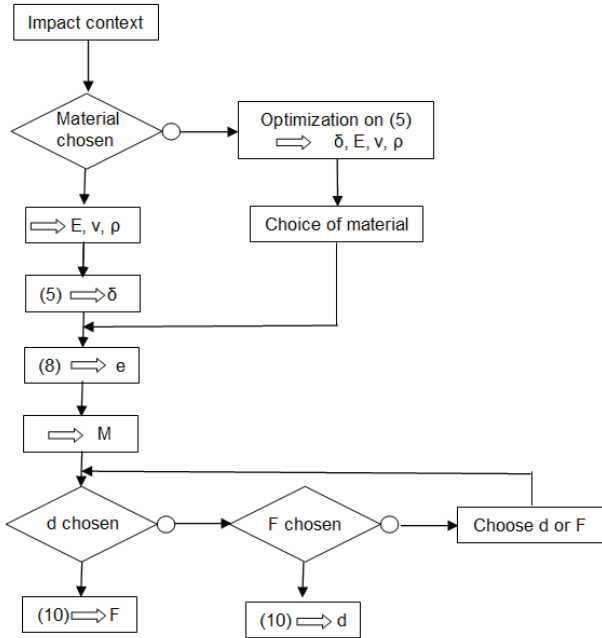

Fig. 3.   Schematic of the algorithm.

E. Algorithm for material, thickness and other parameters determination

Now, considering a given situation of impact (geometrical, inertial and impact parameters known) and a given sensor technology (F_s and S known), we determine the unknown parameters for designing the cover material, E_B being the Young modulus, e the thickness and ρ the density of the skin, and F the minimal detectable force by the sensor and d the resolution of the sensor. We can have some constrains on parameters set by external factors, for instance $d < d_{\max}$ and $F < F_{\max}$, or $e < e_{\max}$. Those constraints must be checked at every step of the algorithm. If not, we have to reconsider the constraints, or to make different choices, namely a different material.

IV. PROTOTYPE

We devised a 1dof motorized arm as a proof-of-concept to perform experiments prior to a first prototype. It is made of a stainless tube attached to the force sensor which in turns is linked to a DC motor. We also realized the tactile matrix, and the polyurethane foam plate on it, see Fig. 4.
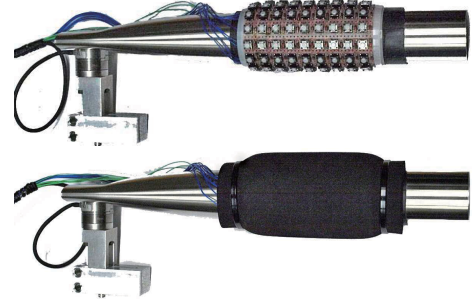

Fig. 4.   Assembled prototype.

A. Design

We took Elastomeric foams as the cover material. This material can extend more than 100% in a classical traction test and remain in the elastic domain. Sensors' screenings and control computation latencies sum to $t_0 \approx 6$ms (we set it to $\tau = 8$ms). The characteristics of arm are $m_B = 0.6$kg, $R_B = 38$mm, $l = 150$mm and $d = 200$mm. The initial speed is $v_0 = 0.4$m.s^{-1} and the contact angle is $\theta_0 = 0$rad. The other constants are $R_{B'} = 38$mm and $g = 9.81$m.s^{-2}.

Our algorithm gives the following solution: $E_B = 3.65 10^5$Pa and $\delta_c = 3.2$mm. We found a material fitting this characteristic thanks to the Matweb database: the micro-cellular polyurethane foam (Young modulus is $E = 3.45\ 10^5$Pa, yield stress is $Y_B = 8.41 10^5$Pa). We changed some values of our device to increase safety $m = 2$kg and $v_0 = 1.5$m.s^{-1}, and use the characteristics of the chosen material in eq. (8); we obtained the following results: $U_r = 4791$J.m^{-3} and $e = 7.90$mm. We found micro-cellular polyurethane foam in 5mm and 10mm thick plate, so we used both as a good approximation of the results of the model, depending of the degree of safety.

In case of sudden contact (switch on), we stop the ongoing motion and reverse it up to the contact detection. We also made an active compliance using the force sensor. We decided of a limit the torque to 3Nm for couple, this value being the rated range of our sensor, which corresponds to

15N for the contact effort, the distance between the sensor and the contact being 20cm.

B. Tactile sheet prototype

We designed a simple matrix of commercial on/off mechanical small switches combined with a force sensor mounted between the link and the actuator; it has 1cm resolution spacing. The keyboard pattern leads to a reduced number of wires that allows a direct connection to the I/O card we used for data processing. In case of an extension of the matrix, i.e. an increase of the number of wires, multiplexing is necessary.

Main computations are done at the same time; to optimize the contact detection time we used a FPGA chip, programmed with VHDL language. These chip and language are particularly designed for task parallelization. The two main tasks are (i) to identify contact zones, i.e. to gather adjacent pressed switches in the same contact set, and (ii) to compute the area and the barycenter of each contact zone.

C. Experiment

We conducted experiments to assess the principle of the system, i.e. detecting the contact and the subsequent in the motion's direction. We also evaluated the efforts resulting from the contact. The experimentation consists in moving the arm into an obstacle. A human arm is used as a sudden obstacle; once detected, the controller reverses the motion, until the contact is resolved, and finally slowing down until its stops.
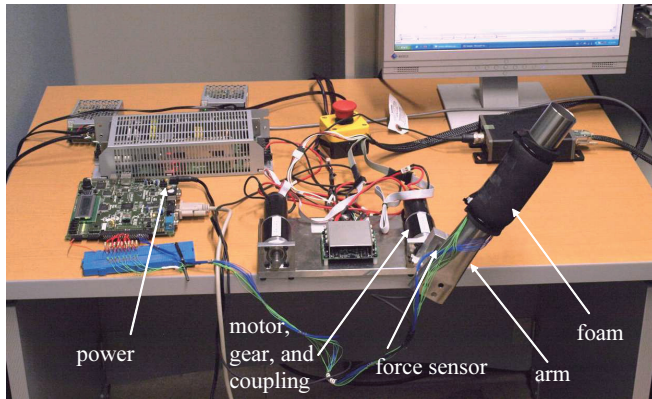

Fig. 5.   Experimental set-up.

We led the experiment with two thicknesses of the flexible foam cover, 5mm and 10mm, the Figs. 6 and 7 show the results of the experiment for the 5mm thick cover. The influence of the thickness is studied further. The Fig. 6 represents the evolution of the angular speed of the arm, and the Fig 7 the evolution of the torque between the arm and the motor.

The Fig. 6 illustrates that the system achieves the previously described behavior. The Fig. 7 shows that the contact is not instantaneously detected, but that the torque, i.e. the contact force, has to reach a certain value for the electrical contact in a switch to be realized.
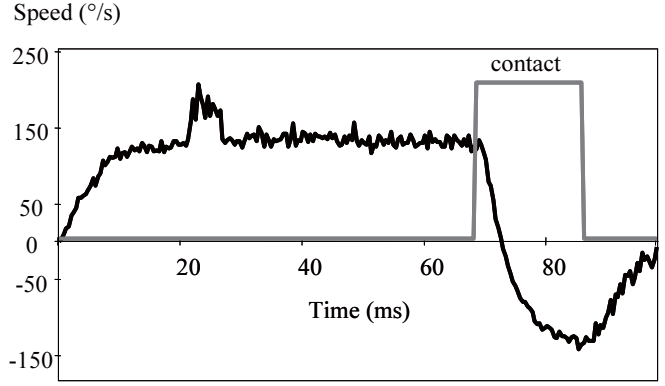

Fig. 6.   Measurement of the speed during the experiment.
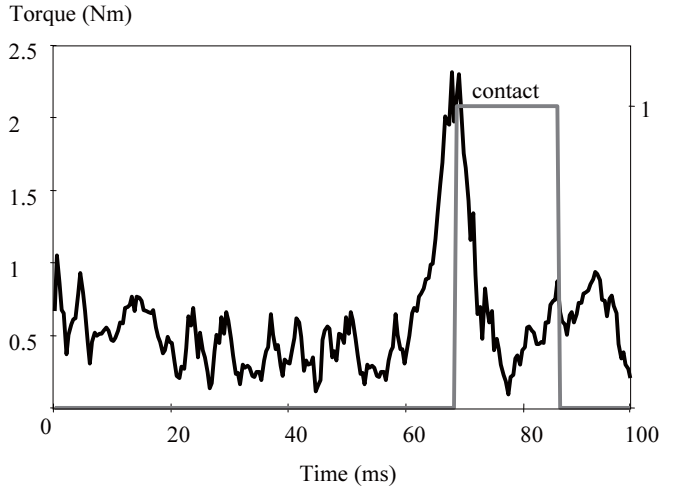

Fig. 7.   Measurement of the torque during the experiment.

The measured values are 2.3Nm for the torque, so 12N for the contact force, the distance between the contact point and the torque sensor being 20cm.

We noted that if the speed starts decreasing as soon as the contact is detected, it stays positive for around 5ms, when the torque immediately decreases, what could be surprising considering that the compression continues as long as the speed is positive. The explanation of this phenomenon is that the measured torque is between the motor and the arm, so when the contact is detected, the reference for the motor immediately changes and the motor tries to go back, when the mechanical inertia of the arm maintains the speed positive for a short time. Indeed the mechanical inertia is higher than the electrical one. It is not really significant in this case, but that point must be kept in mind and taken into account for the next developments of the system.

For our the tactile system we devised, the characteristics of a unit switch are $F_m = 1$N and $S = 12.6 \ 10^{-6}$m^2, $0 < d < 0.005\sqrt{2}$m and $z = 0.005$m, which leads the graphics in Fig. 8.

As we can see on Fig. 8 and from the equation (9), the necessary force to initiate detection grows as a six degree polynomial to $F_c = 65$N for $d = 0.005\sqrt{2}$, i.e. at the
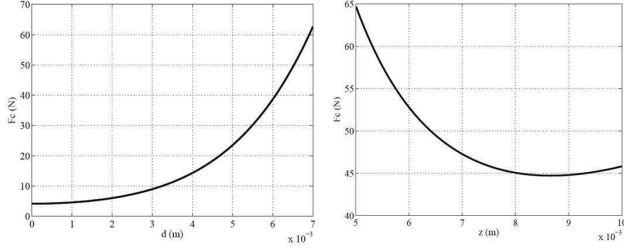
Fig. 8. Contact force in function of the distance for $z = 5$mm and of the thickness for $d = 5\sqrt{2}$mm.

maximum possible distance from a switch.

If we know the force by measurement, as in our experiment described above, we can easily invert this model to evaluate the distance between the contact point and the switch. In our example, we measured $F_c = 12$N, so the value of the distance is $d = 0.0036$m.

We can also see the influence of thickness on the necessary contact force, at the farthest point of any switch, for $d = 0.005\sqrt{2}$m. It shows that in this particular case, the minimal contact force is $F_c = 45$N, equivalent to a 8.5Nm torque at the central point of the force sensor. Considering that the security limit for our force sensor is 3Nm, which stops the system when reached, the maximum contact force acceptable is therefore 15N. It is not possible for it to be detected at $d = 0.005\sqrt{2}$m, as the Fig. 8 showed. From the Fig. 8 and from the equation (9), in the case of a 5mm cover, we find that the maximum distance is $d = 4.2$mm. It means a definition of 5.9mm, as d is the half-diagonal of the square made by the 4 switches around the contact point.

Here this sensitivity study suggests to us to reconsider our initial choice of definition, to ensure contact detection considering the physical limits of the prototype.

D. Linear elastic hypothesis

We run compression tests on our material which led to the results shown on the Fig. 9. This figure shows that the material has an elastic linear behavior up to at least 30N for both thicknesses. The correlation coefficient being superior to 0.99. Therefore, since the maximum measured force in our experiment is 12N, the material remains in the elastic linear domain and the hypothesis made for all computations hold.

V. CONCLUSION

We proposed a simple design to combine at low cost haptic sensing with safe interaction and robust contact formation through outer cover compliance. This system appears to be modular enough to be envisaged as a potential solution to embed haptic sensing and compliance to humanoid robots. We devised a simple one degree of freedom prototype which assesses the feasibility of the idea. We also proposed a method to design the cover and proved it detect collisions and react according to the strategy envisaged for the control. the haptic function combines a flexible sheet of on/off switches
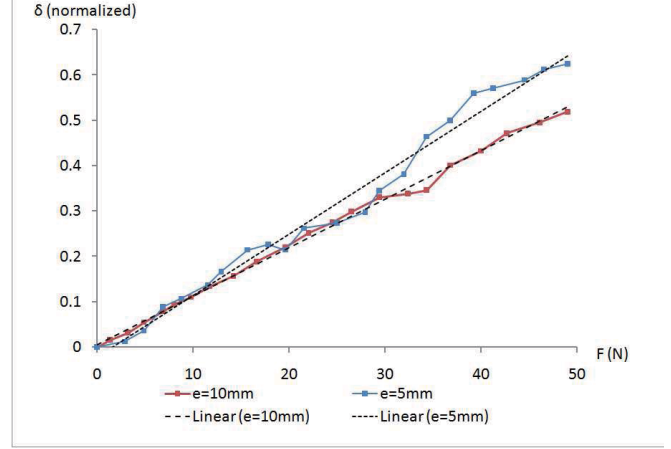

Fig. 9. Deformation in function of the force for both 5mm and 10mm thicknesses.

with a force sensor that could be embedded with a bumper mechanism. It proves the validity of this principle of a tactile soft cover to introduce a safety against collision for the robot and its environment. Furthermore, the sensitivity study gives us valuable information about the possible thickness and definition, considering a limit contact force and a certain kind of switch.

The next step of this work will be to design, on the basis of this principle, a better sensor extensible to a larger area and able to be installed on a real robot, and to solve the problem of sensing at the area of the joint's of the robot.

REFERENCES

[1] A. Kheddar and A. Escande, "Challenges in contact-support planning for acyclic motion of humanoids and androids," in *39th International Symposium on Robotics*, Seoul, Korea, October 15-17 2008, pp. 740–745.

[2] D. Goeger, K. Weiss, C. Burghart, and H. Woern, "Sensitive skin for a humanoid robot," in *Human-Centered Robotic Systems*, Munich, Germany, October 6-7 2006, pp. 115–120.

[3] V. Duchaine, N. Lauzier, M. Baril, M.-A. Lacasse, and C. Gosselin, "A flexible robot skin for safe physical human robot interaction," in *IEEE International Conference on Robotics and Automation*, Kobe, Japan, May 12-17 2009, pp. 3676–3681.

[4] X. Lamy, F. Colledani, F. Geffard, Y. Measson, and G. Morel, "Robotic skin structure and performances for industrial robot comanipulation," in *IEEE/ASME International Conference on Advanced Intelligent Mechatronics*, Singapore, July 14-17 2009, pp. 427–432.

[5] A. Nagakubo, H. Alirezaei, and Y. Kuniyoshi, "A deformable and deformation sensitive tactile distribution sensor," in *IEEE International Conference on Robotics and Biomimetics*, Sanya, China, December 15-18 2007, pp. 1301–1308.

[6] T. Sugaiwa, H. Iwata, and S. Sugano, "Shock absorbing skin design for human-symbiotic robot at the worst case collision," in *IEEE-RAS International Conference on Humanoid Robots*, Daejeon, Korea, December 1-3 2008, pp. 481–486.

[7] S. Haddadin, A. Albu-Schaeffer, M. Frommberger, J. Rossmann, and G. Hirzinger, "The DLR crash report: towards a standard crash-testing protocol for robot safety - part I and II," in *IEEE International Conference on Robotics and Automation*, Kobe, Japan, May 12-17 2009, pp. 272–287.

[8] W. J. Stronge, *Impact mechanics*. Cambridge University Press, 2000.

[9] K. L. Johnson, *Contact mechanics*. Cambridge University Press, 1985.